Electron-impact cross sections and coherence parameters for the $6s^2\,{}^1S-6s6p\,{}^1P$ transition in neutral barium

R. E. H. Clark, J. Abdallah, Jr., G. Csanak, and S. P. Kramer
Los Alamos National Laboratory, Los Alamos, New Mexico 87545
(Received 31 March 1989)

Integral and differential cross sections and electron-impact coherence parameters have been calculated for the $6s^2\,{}^1S-6s6p\,{}^1P$ transition in neutral barium using both the distorted-wave approximation and first-order many-body theory. Target-state wave functions have been calculated using Hartree-Fock orbitals along with configuration-interaction and intermediate-coupling mixing. Results are presented for electron-impact energies of 5, 10, 15, 20, 30, 40, 60, 80, and 100 eV. The cross sections are compared to available experimental and theoretical results.

I. INTRODUCTION

The electron-impact excitation of barium is of considerable scientific interest. The main reason for this is that barium is one of the few atoms that can be efficiently pumped by currently available laser systems and thus photoabsorption, photoionization, and electron collision experiments can be performed on laser-excited barium atoms.[1–9] The study of electron-impact excitation and deexcitation from excited atomic systems is in turn of both scientific and practical interests since such processes are important in naturally occurring and laboratory-produced plasmas.[10–13] The physics of such processes is barely understood due to the very few experimental and theoretical studies that have been done in this area. In the case of barium, however, some experimental results have already been reported for electron-impact excitation and deexcitation cross sections from several excited states at a few energies and angles[7] as well as for electron-impact ionization of two excited states of barium.[8] In the case of the excitation-deexcitation study from the $6s6p\,{}^1P_1$ state[7] the normalization of the intensity data was accomplished by utilizing the principle of detailed balance for the $6s6p\,{}^1P_1\rightarrow 6s^2\,{}^1S_0$ transition along with inelastic excitation cross-section data for the $6s^2\,{}^1S_0\rightarrow 6s6p\,{}^1P_1$ transition obtained earlier.[14] The normalization of the $6s^2\,{}^1S_0\rightarrow 6s6p\,{}^1P_1$ inelastic scattering cross sections in turn was based on the optical excitation function measurements of Chen and Gallagher,[15] that superseded the first measurement by Aleksakhin *et al.*[16] of the optical excitation function of the Ba resonance line, and resulted in an estimated error of $\pm 50\%$. This latter normalization procedure was based, however, on two rather uncertain assumptions: (i) the apparent cross sections obtained in the optical excitation function measurement[15] were decreased arbitrarily by 30% to account for cascade and (ii) the measured differential cross sections were interpolated to intermediate angles and extrapolated to zero scattering angle. As the authors point out[14] the extrapolation procedure, especially for angles below 5°, may not be accurate.

In view of the great importance of the $6s^2\,{}^1S_0\rightarrow 6s6p\,{}^1P_1$ transition for normalization purposes and the rather large uncertainty for normalizing the experimental differential cross section for this transition we might assume that theoretical calculations may be helpful for normalizing the experimental data. The only theoretical calculations reported so far for Ba excitation are those of Fabrikant,[17,18] and Damburg and Fabrikant,[19] which used the close-coupling scheme. Two of these calculations[17,19] were performed for energies close to the threshold and only the third[18] reported differential cross sections for the $6s^2\,{}^1S_0\rightarrow 6s6p\,{}^1P_1$ excitation at 20 and 30 eV incident electron energies that could be compared with the available experimental results.[14] This latter work[18] used a two-state $\{6\,{}^1S_0, 6\,{}^1P_1\}$ close-coupling scheme along with semiempirical wave functions and ignoring electron exchange between the incident electron and the core electrons of the target. Fabrikant[17] also showed that for the calculation of the $6\,{}^1P_1$ excitation cross section, the coupling to the ^1D state is negligible for $E>8$ eV incident electron energies. Thus it appeared worthwhile to put the calculation of electron-impact scattering cross sections for a barium target on a sound theoretical foundation and one of the purposes of the present work is to report distorted-wave approximation (DWA) results using the approach of Mann,[20] and first-order many-body theory (FOMBT) results for the $6\,{}^1S_0\rightarrow 6\,{}^1P_1$ excitation process.

Our procedure uses *ab initio* wave functions, and electron exchange is fully taken into account. In the past, the DWA and FOMBT have been used successfully for the calculation of $n\,{}^1P$ electron-impact cross sections for He (Refs. 21–26) and Mg targets[27] for intermediate energy incident electrons. The FOMBT results[27] for $3\,{}^1P$ excitation of Mg agree well with the experimental results[28,29] at 20 and 40 eV incident energies for $\theta<30°$ scattering angles.

An additional significance of theoretical calculations for the electron-impact excitation of the $6s6p\,{}^1P_1$ state of barium is that the $6s6p\,{}^1P_1$ state can be pumped efficiently by *polarization selected* laser beams.[30] This opens up the possibility of measuring the electron-impact coherence parameters for the $6s^2\,{}^1S_0\rightarrow 6s6p\,{}^1P_1$ electron-impact excitation process,[31] a technique introduced by Hertel and Stoll[32,33] and applied successfully to

TABLE I. Calculated f values and transition energies.

Configurations included in ground state	Configurations included in excited state	f	ΔE (eV)
$6s^2$	$6s6p$	3.36	2.385
$6s^2, 6p^2$	$6s6p, 5d6p$	1.63	2.046
$6s^2, 6p^2, 5d^2$, $6s7s, 6p7p$	$6s6p, 5d6p, 6s7p$,	2.03	2.112

various transitions in sodium.[34-38] Unfortunately, when this technique was tried for Ba, an undesired and inexplicable asymmetry effect[39] prevented the experimentalists from extracting quantitative information from the experimental results. However, recent modeling studies along with new observations and the theoretically obtained electron-impact coherence parameters (EICP's) from the same studies reported here appear to have clarified the situation[40] and opened the way for meaningful experiments. Thus we report here EICP's for the $6s^2\,{}^1S_0 \rightarrow 6s6p\,{}^1P_1$ excitation of Ba. One of the significant results of the present calculations was that while all EICP's relevant for spin-orbit coupled target states were calculated, namely, the $\lambda, \bar{\chi}, \cos\epsilon, \cos\Delta$ of da Paixão *et al.*,[41] it was found that at the energies considered $\cos\epsilon$ and $\cos\Delta$ are equal to 1 within our numerical accuracy and thus a completely LS-coupled situation obtains,[38,41] similar to the He $1\,{}^1S \rightarrow n\,{}^1P$ excitation process and thus we shall report here only the λ and χ parameters as defined by Eminyan *et al.*[42] at selected energies.

II. METHOD OF CALCULATION

The present calculations were performed using a set of codes developed at the Los Alamos National Laboratory as part of a Theoretical Atomic Physics[43-46] code development effort. These codes have recently been used to calculate optical and electron-impact collision strength data for all ion stages of nitrogen.[47] We shall briefly summarize here the operation and function of these codes that we used in the present study.

Atomic structure calculations are performed with the CATS code,[43] a modified version of Cowan's atomic structure codes.[48-51] The atomic structure calculation is initiated with a single-configuration Hartree-Fock calculation (Cowan's HFR) for the radial wave functions of each configuration. It is essentially a nonrelativistic calculation except that the mass and Darwin terms are included in the radial wave function calculation. The radial wave functions minimize the configuration-average energy, not the LS-term energy. Mixing among all configurations and LS terms with the same total angular momentum, J, and parity is then obtained through perturbation theory. Results from the structure calculation are stored on a random access computer file. Data stored on the file include a list of configurations with the configuration-average energies and radial wave functions, mixing coefficients, fine-structure energy levels and oscillator strengths. If requested, plane-wave Born (PWB) collision strengths and photoionization cross sections may also be calculated and stored.

Data stored on the computer file can be viewed with the TAPS code.[45] Various data can be summed or averaged to form term-to-term or configuration-to-configuration quantities. Data can be listed at the terminal, plotted as a graph when appropriate or sent to a print file. The radial wave functions can be used to calculate and display the electron charge density and potential as functions of the radial distance. The LINES code[46] can be used to display data and to calculate populations in the local thermodynamic equilibrium (LTE) condition at a given temperature and density and calculate and display a synthetic spectrum.

The electron collision calculations are performed using the ACE code.[44] This code reads in data from the atomic structure file and calculates electron-impact collision strengths using a variety of options. The collision strengths can be converted to cross sections using the TAPS code. The ACE code uses the distorted-wave approximation of Mann,[20] or first-order many-body theory.[52,53] The only difference between the DWA and FOMBT calculations is that in the former case (DWA), we calculate the continuum wave function in the potential of the initial and final configurations for the incident and scattered electron, respectively, whereas in the latter case (FOMBT), the same potential (that of the initial configuration) is used for both continuum electrons. The procedure used in the DWA is considered physically more appealing (the scattered electron moves in the field of the final configuration), whereas the FOMBT has the advantage that since the initial and final continuum wave functions are obtained from the same potential (at different energies) they are orthogonal. The bound-state radial wave functions are normally the HFR wave functions of Cowan[51] but can be calculated purely hydrogenically via in-line subroutines for comparison purposes. The continuum wave functions are normally calculated

TABLE II. Integral cross sections in units of πa_0^2.

E (eV)	Q (DWA)	Q (FOMBT)
5.0	45.2	51.2
10.0	60.3	61.4
15.0	58.0	58.8
20.0	57.1	56.7
30.0	48.0	48.3
40.0	41.3	41.7
60.0	32.6	32.8
80.0	27.1	27.3
100.0	23.3	23.5

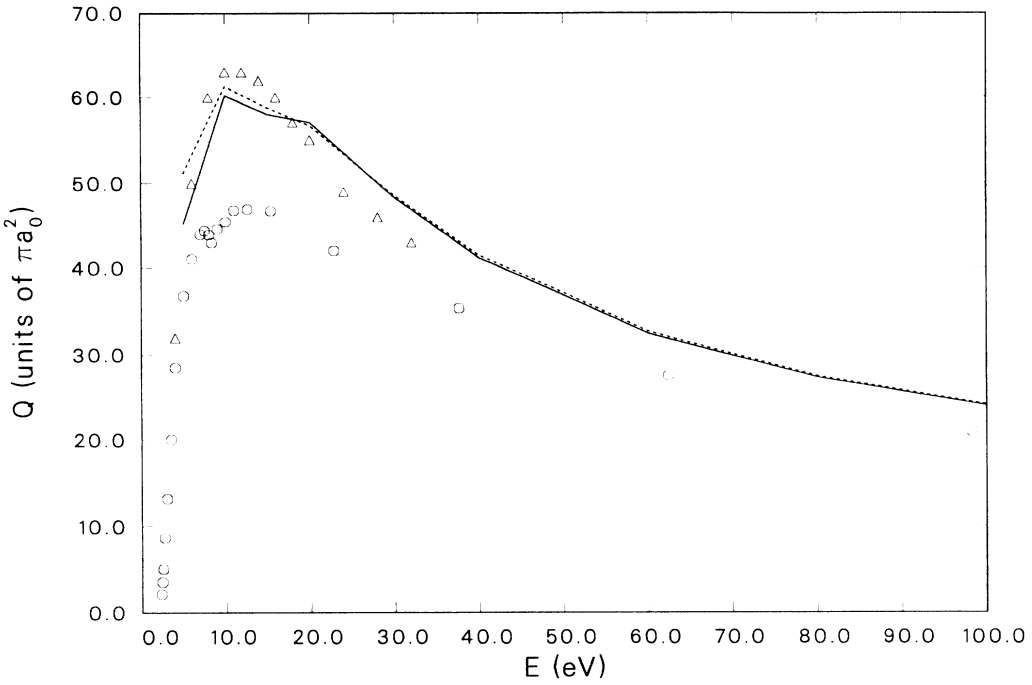

FIG. 1. Comparison of integral cross sections: ——, DWA; — — —, FOMBT; △, Fabrikant (Ref. 18); ○, Chen and Gallagher (Ref. 15).

using the DWA of Mann.[20] The continuum wave function can also be calculated using FOMBT (Refs. 52 and 53) or it can be a Coulomb function, in the case of an ion, using in-line subroutines. The reactance matrix elements are first calculated between *LS* terms as in Mann's[20] approach. Unitarization of the reactance matrix is normally carried out; however, unitarization can be ignored for comparison purpose (see Sec. III for integral cross-section comparisons in barium). Recoupling is then done using the pair coupling scheme of Saraph:[54]

$$\mathbf{J}_a+\mathbf{s}=\mathbf{K}, \quad \mathbf{K}+l=\mathbf{J}_T , \tag{1}$$

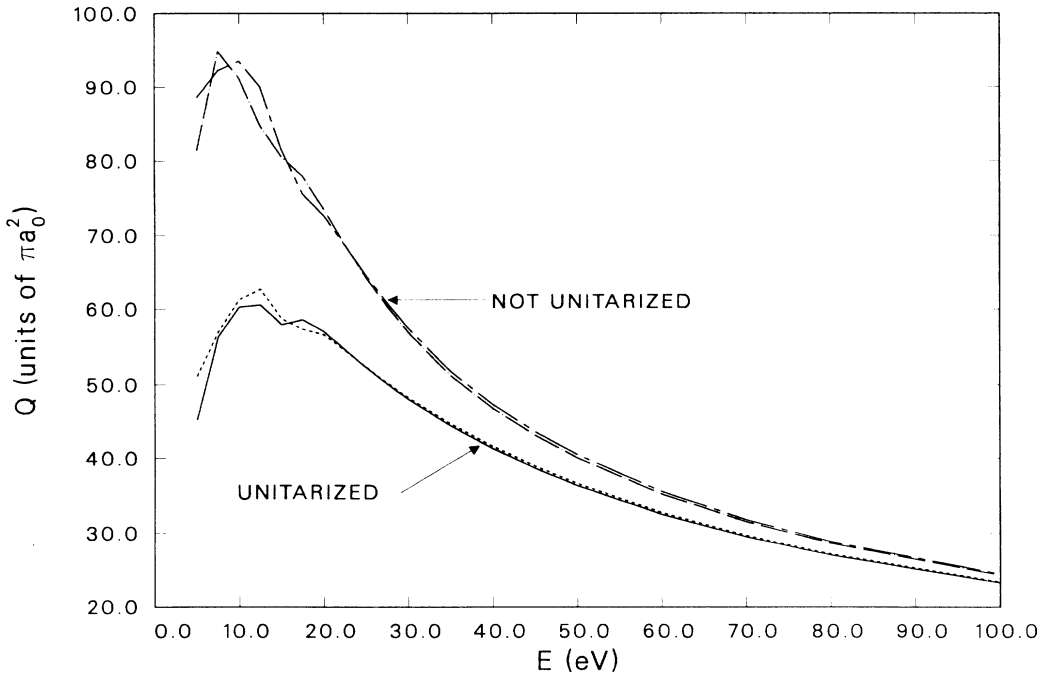

FIG. 2. Comparison of integral cross sections with and without unitarization: ——, DWA unitarized; —·—·—·, DWA not unitarized; — — —, FOMBT unitarized; —·—·, FOMBT not unitarized.

TABLE III. Number of partial waves used at each energy.

E (eV)	l_{max}
5.0	100
10.0	100
15.0	100
20.0	100
30.0	250
40.0	250
60.0	250
80.0	300
100.0	300

where $\mathbf{J}_a$ is the angular momentum vector of the atom, s is the spin angular momentum vector of the free electron, l is the orbital angular momentum vector of the free electron, and $\mathbf{J}_T$ is the total angular momentum vector of the system. This coupling scheme effectively replaces each 9-j symbol[55] of Mann's[20] recoupling scheme with two 6-j symbols. Inclusion of configuration-interaction and intermediate-coupling mixing is obtained as by Clark.[56] It should be emphasized that the continuum wave functions are calculated with no mixing, i.e., with each configuration there is an associated continuum wave function. The mixing is carried out later in the reactance matrix elements.

If desired, the user can request differential cross sections (DCS's) from the ACE code. The ACE code then uses the reactance matrix along with continuum wave function phases to calculate the (complex) scattering amplitudes using the recoupling scheme of Inal and Dubau.[57] The scattering amplitude is stored on a data file and can be used to calculate DCS's and electron-impact coherence parameters via the TAPS code.[45] We note that the phase used in the calculation of the scattering amplitude uses the mixing coefficients and the phases of the unmixed continuum wave functions:

$$\delta_{\text{mix}} = \sum_{i=1}^{N_{\text{config}}} a_i^2 \delta_i \ , \tag{2}$$

where δ_i is the phase and a_i is the mixing coefficient. In barium, the phases calculated from the different configurations are not very different so that the scattering amplitudes calculated using Eq. (2) do not differ noticeably from those calculated with phases purely from the dominant configurations involved in the transition (the $6s^2$ and $6s6p$ configurations). For example, the phases arising from the $6s6p$ configuration are within 0.1 rad of those arising from the $5d6p$ configuration.

III. NUMERICAL RESULTS

The CATS code[43] was used to calculate energy levels and oscillator strengths for the $6s^2\,{}^1S_0$–$6s6p\,{}^1P_1$ transition using varying set of configurations. Results are shown in Table I. Parkinson, Reeves, and Tomkins[58] report $f = 1.59 \pm 0.15$ which is identical to the value reported by Miles and Wiese.[59] The observed transition energy is 2.239 eV. One sees from Table I that all the calculations give the transition energy correct to within 0.2 eV. However, the oscillator strength calculated with only a single configuration for the ground and excited states is in error by a factor of 2. Including the $6p^2$ and $5d6p$ configurations greatly improves the oscillator strength, while using five configurations each for the ground and excited states makes little change ($\sim 25\%$ in the f value) and, in fact, gives slightly poorer agreement with the observed value. We have therefore used the $6s^2$, $6p^2$, $6s6p$, and $5d6p$ configurations in the structure calculations used in the excitation cross sections reported here.

We now consider integral cross-section calculations. The ACE code normally adds and subtracts the PWB collision strength so that the total collision strength is given by (for DWA; similarly for FOMBT):

$$\Omega = \Omega^{\text{PWB}} + \sum_{l=0}^{\infty} (\Omega_l^{\text{DW}} - \Omega_l^{\text{PWB}}) \ , \tag{3}$$

where the subscript l denotes the partial wave contribution. The collision strength and cross section are related by

$$Q = \frac{\pi a_0^2}{\omega_i [E(\text{Ry})]} \Omega \ , \tag{4}$$

where Q is the cross section, ω_i is the statistical weight of the initial state, E(Ry) is the impact electron energy in rydbergs, and Ω is the collision strength. The ACE code actually calculates collision strengths; the TAPS code will display either collision strengths or cross sections using Eq. (4) as requested. In practice, $\Omega_l^{\text{DW}} \rightarrow \Omega_l^{\text{PWB}}$ for finite l so that the sum in Eq. (3) can be terminated at a finite value, l_{max}. Thus, only a limited number of partial waves need be calculated.

Using $l_{max} = 20$ usually gives results converged to less than 5% at all energies and normally less than 2%. We note that the transformation analogous to Eq. (3) has not yet been implemented in the differential cross section (DCS) calculations. Thus large numbers of partial waves must be used for the DCS calculation. The integral cross sections from those calculations can be compared to those calculated via Eqs. (3) and (4) to check for convergence.

In Table II we present our integral cross section results for nine energies between 5 and 100 eV. Calculations were performed using both the DWA and FOMBT approaches and using the unitarization procedure. The results are shown graphically in Fig. 1 where they are compared with experimental values of Chen and Gallagher.[15] Also shown are theoretical results from a close-coupling calculation by Fabrikant.[18]

The DWA and FOMBT results shown in Table II and Fig. 1 were calculated using the unitarized reactance matrix. To show the effect of unitarization, we repeated the calculations without the unitarization procedure. The results are shown graphically in Fig. 2. The unitarization of the reactance matrix lowers the integral cross section by nearly a factor of 2 at energies around 10 eV. The effect diminishes at higher energies, to around a 5% effect at 100 eV.

TABLE IV. Differential cross sections in units of πa_0^2 calculated in the distorted-wave approximation (DWA). Column headings are electron-impact energies. Numbers in square brackets represent powers of 10.

θ \ E (eV)	5.0000	1.0000[1]	1.5000[1]	2.0000[1]	3.0000[1]	4.0000[1]	6.0000[1]	8.0000[1]	1.0000[2]
0.0000	1.1671[2]	6.0108[2]	1.2400[3]	1.9941[3]	3.7679[3]	3.9443[3]	8.1746[3]	1.2017[4]	1.7828[4]
5.0000	1.0383[2]	3.8850[2]	5.0493[2]	5.4342[2]	4.4674[2]	3.5325[2]	2.3425[2]	1.5967[2]	1.1263[2]
1.0000[1]	7.2068[1]	1.4747[2]	1.2769[2]	1.0936[2]	6.6283[1]	4.2969[1]	2.0304[1]	1.0629[1]	5.6607
1.5000[1]	4.2655[1]	5.1225[1]	3.4145[1]	2.5447[1]	1.2822[1]	7.2266	3.0722	1.8062	1.0515
2.0000[1]	2.2427[1]	1.7907[1]	1.0212[1]	6.5928	3.3751	2.2333	1.3369	8.3321[−1]	5.3720[−1]
2.5000[1]	1.0780[1]	7.0473	4.2382	2.0905	1.4849	1.1987	7.1781[−1]	4.1847[−1]	2.5815[−1]
3.0000[1]	4.8580	3.6783	2.8675	1.0963	8.2695[−1]	6.7293[−1]	3.8016[−1]	1.9554[−1]	1.1202[−1]
3.5000[1]	2.2389	2.6079	2.5324	9.5801[−1]	5.5285[−1]	3.7706[−1]	1.5779[−1]	6.6546[−2]	3.3560[−2]
4.0000[1]	1.3006	2.1866	2.3531	1.0445	4.3666[−1]	2.1460[−1]	5.4068[−2]	2.3900[−2]	2.1547[−2]
4.5000[1]	1.1397	1.9316	2.0964	1.1396	4.0456[−1]	1.4964[−1]	2.4207[−2]	1.9898[−2]	2.6485[−2]
5.0000[1]	1.2699	1.7288	1.7259	1.0967	3.6874[−1]	1.1293[−1]	1.7276[−2]	2.2670[−2]	2.4695[−2]
5.5000[1]	1.4655	1.5535	1.2934	9.0984[−1]	3.0421[−1]	7.8858[−2]	1.9152[−2]	2.8197[−2]	2.4203[−2]
6.0000[1]	1.6202	1.3916	8.9138[−1]	6.9012[−1]	2.2072[−1]	4.7794[−2]	1.9083[−2]	3.1593[−2]	2.5608[−2]
6.5000[1]	1.6928	1.2344	5.7549[−1]	4.9317[−1]	1.4338[−1]	2.4486[−2]	1.5896[−2]	2.5260[−2]	2.2714[−2]
7.0000[1]	1.6642	1.0831	3.7787[−1]	3.4151[−1]	9.4052[−2]	1.3699[−2]	8.6069[−3]	1.6194[−2]	1.8466[−2]
7.5000[1]	1.5527	9.4127[−1]	2.9396[−1]	2.5913[−1]	7.9898[−2]	1.6919[−2]	3.4531[−3]	1.0837[−2]	1.7603[−2]
8.0000[1]	1.3822	8.1824[−1]	2.9376[−1]	2.4851[−1]	1.0543[−1]	3.4654[−2]	1.7655[−3]	8.4920[−3]	1.8506[−2]
8.5000[1]	1.1989	7.1650[−1]	3.2200[−1]	2.8854[−1]	1.5285[−1]	6.1592[−2]	2.3085[−3]	8.7335[−3]	2.0981[−2]
9.0000[1]	1.0494	6.3106[−1]	3.3523[−1]	3.3215[−1]	2.1549[−1]	9.3167[−2]	4.1300[−3]	1.0137[−2]	2.5514[−2]
9.5000[1]	9.7730[−1]	5.5891[−1]	3.1128[−1]	3.6077[−1]	2.6892[−1]	1.2554[−1]	8.7367[−3]	9.0279[−3]	2.5766[−2]
1.0000[2]	1.0128	4.9447[−1]	2.4947[−1]	3.6094[−1]	3.1428[−1]	1.5887[−1]	1.8790[−2]	5.9757[−3]	1.5938[−2]
1.1000[2]	1.4094	3.9463[−1]	1.0255[−1]	2.4066[−1]	3.3122[−1]	2.1175[−1]	5.9650[−2]	1.4604[−2]	2.7880[−3]
1.2000[2]	2.0431	3.9071[−1]	1.2927[−1]	8.0583[−2]	2.5671[−1]	2.1790[−1]	9.7112[−2]	3.1984[−2]	7.3266[−3]
1.3000[2]	2.5337	5.5217[−1]	3.5111[−1]	1.4254[−2]	1.1998[−1]	1.5211[−1]	9.2221[−2]	3.2317[−2]	9.2654[−3]
1.4000[2]	2.5963	8.8897[−1]	5.7335[−1]	1.3934[−1]	1.1721[−2]	4.6456[−2]	4.2885[−2]	1.1653[−2]	3.0371[−4]
1.5000[2]	2.2180	1.3195	6.0703[−1]	5.0698[−1]	6.9259[−2]	2.7172[−2]	4.3168[−2]	3.7590[−2]	2.7812[−2]
1.6000[2]	1.6194	1.7308	4.8395[−1]	1.0866	3.4269[−1]	1.7944[−1]	1.7811[−1]	1.7350[−1]	1.3299[−1]
1.7000[2]	1.1051	2.0067	3.3441[−1]	1.6342	6.8881[−1]	4.1627[−1]	3.8936[−1]	3.6165[−1]	2.8471[−1]
1.8000[2]	9.0133[−1]	2.1023	2.7526[−1]	1.8430	8.6117[−1]	5.2754[−1]	4.9113[−1]	4.6145[−1]	4.0892[−1]

TABLE V. Differential cross sections in units of πa_0^2 calculated in the first-order many-body theory approximation (FOMBT). Column headings are electron-impact energies. Numbers in square brackets represent powers of 10.

θ \ E (eV)	5.0000	1.0000[1]	1.5000[1]	2.0000[1]	3.0000[1]	4.0000[1]	6.0000[1]	8.0000[1]	1.0000[2]
0.0000	1.1135[2]	6.0500[2]	1.2089[3]	2.0246[3]	3.8286[3]	4.0074[3]	8.2559[3]	1.2102[4]	1.7917[4]
5.000	9.8843[1]	3.8929[2]	4.9095[2]	5.4766[2]	4.5169[2]	3.5685[2]	2.3638[2]	1.6102[2]	1.1351[2]
1.0000[1]	6.8011[1]	1.4586[2]	1.2374[2]	1.0743[2]	6.5657[1]	4.2696[1]	2.0197[1]	1.0583[1]	5.6362
1.5000[1]	3.9800[1]	4.9541[1]	3.3758[1]	2.3687[1]	1.2076[1]	6.8926	2.9682	1.7353	1.0098
2.0000[1]	2.0817[1]	1.6894[1]	1.1180[1]	5.8090	3.0451	2.1460	1.3620	8.6386[−1]	5.6911[−1]
2.5000[1]	1.0264[1]	6.6895	5.4663	1.9979	1.4452	1.2329	7.5112[−1]	4.3764[−1]	2.7302[−1]
3.0000[1]	5.1744	3.7550	3.8150	1.3174	9.1752[−1]	7.2993[−1]	3.9289[−1]	1.9497[−1]	1.1151[−1]
3.5000[1]	3.0893	2.8908	3.0172	1.2538	6.8100[−1]	4.3237[−1]	1.6603[−1]	7.1103[−2]	3.9089[−2]
4.0000[1]	2.4009	2.5157	2.4364	1.2752	5.4128[−1]	2.5727[−1]	6.5343[−2]	3.1140[−2]	2.7243[−2]
4.5000[1]	2.2653	2.2137	1.9551	1.2409	4.6817[−1]	1.7635[−1]	3.3228[−2]	2.6191[−2]	3.0646[−2]
5.0000[1]	2.2753	1.9231	1.5613	1.0864	3.9052[−1]	1.2457[−1]	2.4170[−2]	2.8563[−2]	2.9093[−2]
5.5000[1]	2.2794	1.6600	1.2409	8.3732[−1]	3.0149[−1]	8.2984[−2]	2.4425[−2]	3.2357[−2]	2.7301[−2]
6.0000[1]	2.2264	1.4357	9.9087[−1]	6.0411[−1]	2.0945[−1]	4.9112[−2]	2.1011[−2]	3.2133[−2]	2.5838[−2]
6.5000[1]	2.1085	1.2503	7.8844[−1]	4.2507[−1]	1.3391[−1]	2.5609[−2]	1.6102[−2]	2.4019[−2]	2.1426[−2]
7.0000[1]	1.9224	1.1036	6.3279[−1]	3.0151[−1]	9.0807[−2]	1.5852[−2]	8.6344[−3]	1.5497[−2]	1.7759[−2]
7.5000[1]	1.6642	9.9143[−1]	5.2642[−1]	2.4440[−1]	8.0917[−2]	1.9440[−2]	3.8149[−3]	1.0821[−2]	1.7773[−2]
8.0000[1]	1.4156	9.0838[−1]	4.7454[−1]	2.4347[−1]	1.0690[−1]	3.6511[−2]	2.0156[−3]	8.6723[−3]	1.9130[−2]
8.5000[1]	1.1525	8.4534[−1]	4.6311[−1]	2.7273[−1]	1.4985[−1]	6.1466[−2]	2.4294[−3]	8.7266[−3]	2.1324[−2]
9.0000[1]	9.4340[−1]	7.8764[−1]	4.7302[−1]	2.9971[−1]	2.0498[−1]	9.0658[−2]	4.4478[−3]	9.7970[−3]	2.4789[−2]
9.5000[1]	8.3915[−1]	7.2834[−1]	4.7938[−1]	3.1077[−1]	2.5042[−1]	1.2022[−1]	9.4649[−3]	8.9113[−3]	2.4722[−2]
1.0000[2]	8.8556[−1]	6.6499[−1]	4.5749[−1]	3.0009[−1]	2.8865[−1]	1.5069[−1]	1.9690[−2]	6.6805[−3]	1.5950[−2]
1.1000[2]	1.5046	5.5789[−1]	3.0914[−1]	1.8646[−1]	2.9999[−1]	1.9811[−1]	5.8054[−2]	1.4651[−2]	2.9480[−3]
1.2000[2]	2.6729	5.8481[−1]	1.7646[−1]	5.8835[−2]	2.2877[−1]	2.0065[−1]	9.3082[−2]	3.1621[−2]	7.5618[−3]
1.3000[2]	3.8611	8.1434[−1]	2.5384[−1]	2.6850[−2]	1.0416[−1]	1.3627[−1]	8.6135[−2]	3.0662[−2]	8.3803[−3]
1.4000[2]	4.4543	1.1650	5.2934[−1]	1.6217[−1]	1.2600[−2]	4.1215[−2]	4.0312[−2]	1.1372[−2]	4.3811[−4]
1.5000[2]	4.1494	1.4461	7.4225[−1]	4.7551[−1]	6.9157[−2]	2.4402[−2]	4.0519[−2]	3.6534[−2]	2.7367[−2]
1.6000[2]	3.1622	1.5357	6.9915[−1]	9.1790[−1]	3.0602[−1]	1.5415[−1]	1.5944[−1]	1.6098[−1]	1.2614[−1]
1.7000[2]	2.1245	1.4811	4.6890[−1]	1.3109	5.9771[−1]	3.5315[−1]	3.3859[−1]	3.3183[−1]	2.6684[−1]
1.8000[2]	1.6910	1.4329	3.3997[−1]	1.4644	7.5110[−1]	4.5229[−1]	4.3829[−1]	4.3222[−1]	3.9167[−1]

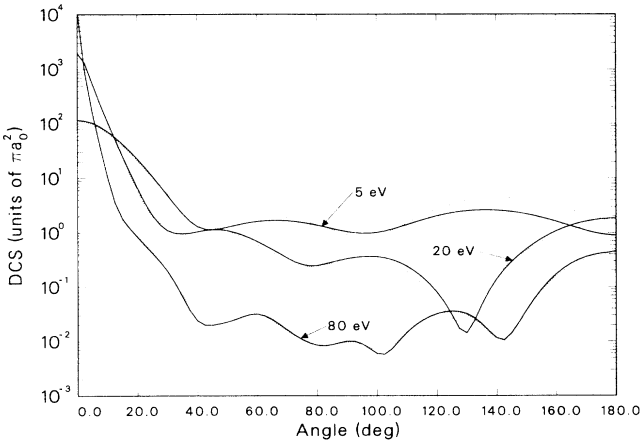

FIG. 3. Comparison of differential cross sections using DWA (solid line) and FOMBT (dotted line) at 5, 20, and 80 eV.

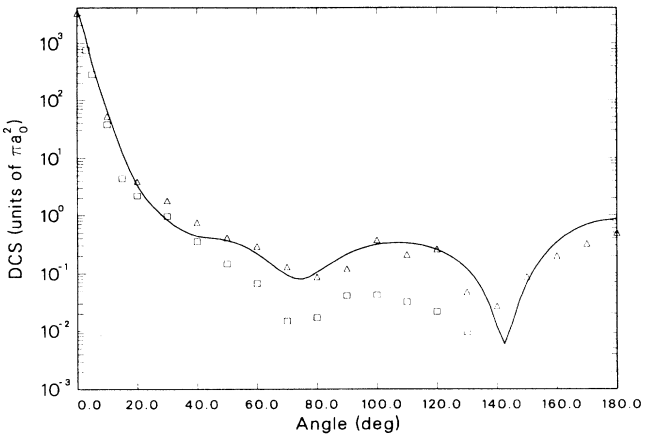

FIG. 5. Comparison of DCS's calculated with DWA (solid line) with experimental results of Jensen *et al.* (Ref. 14) (squares), and close-coupling results of Fabrikant (Ref. 18) (triangles) at electron-impact energy of 30 eV.

As mentioned above, the convergence technique of Eq. (3) has not been implemented in the differential cross-section calculation. Thus we have computed the DCS values using enough partial waves to give $\sim 1\%$ convergence of the integral cross section at each energy. Table III shows the maximum partial wave used at each energy. In Tables IV and V we present DCS calculation results using the DWA and FOMBT approaches, respectively, at representative angles for nine energies between 5 and 100 eV. Figure 3 shows comparison plots of the DCS calculations using DWA (solid line) and FOMBT (dotted line) at 5, 20, and 80 eV. The DWA and FOMBT show maximum difference at low energies and angles greater than 20°. At 80 eV, the two calculations are nearly identical.

In Figs. 4–9, we compare our DWA results with the experimental results of Jensen *et al.*[14] and the close-coupling results of Fabrikant[18] (available at 20 and 30 eV only) for impact electron energies of 20, 30, 40, 60, 80, and 100 eV. In all cases the solid line represents our DWA results, the squares represent those of Jensen *et al.*,[14] and the triangles represent those of Fabrikant.[18] At 20 and 30 eV our DWA results are in good agreement with Fabrikant's calculations; both sets of theoretical calculations are significantly above the experimental values for angles greater than 40°. At higher energies, the DWA results agree quite well with the experimental values.

In the calculation of the EICP's we again point out that the $\cos\epsilon$ and $\cos\Delta$ parameters[38,41] are equal to 1 within numerical accuracy implying a nearly completely *LS*-coupled situation. It is instructive to view this also in terms of the mixing coefficients of the excited target state. The excited state is a mixture of the two configurations $6s6p$ and $5d6p$. The $6s6p\ ^1P_1$ level is made up of the following mixture:

$$\psi_{6s6p\ ^1P_1} = 0.812\psi^0_{6s6p\ ^1P_1} - 0.579\psi^0_{5d6p\ ^1P_1} - 0.057\psi^0_{6s6p\ ^3P_1}$$

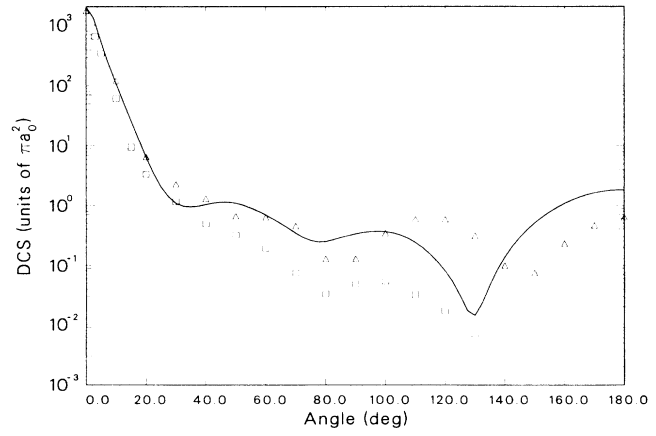

FIG. 4. Comparison of DCS's calculated with DWA (solid line) with experimental results of Jensen *et al.* (Ref. 14) (squares), and close-coupling results of Fabrikant (Ref. 18) (triangles) at electron-impact energy of 20 eV.

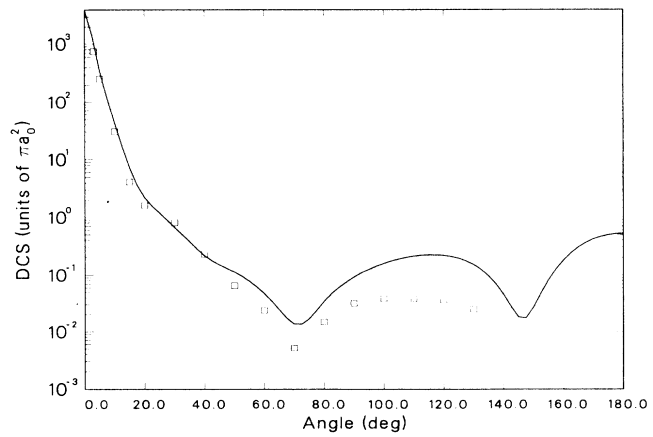

FIG. 6. Comparison of DCS's calculated with DWA (solid line) with experimental results of Jensen *et al.* (Ref. 14) (squares) at 40 eV.

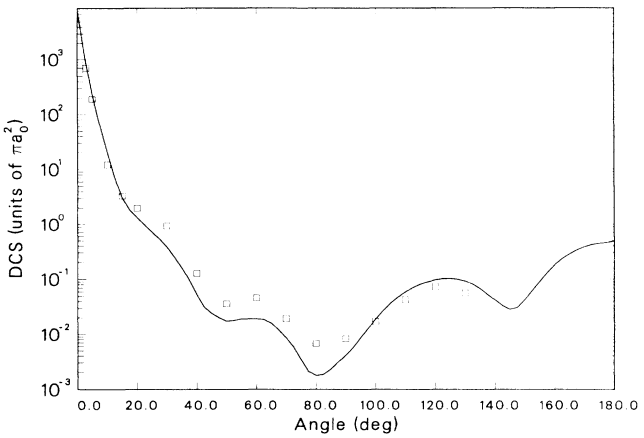

FIG. 7. Comparison of DCS's calculated with DWA (solid line) with experimental results of Jensen *et al.* (Ref. 14) (squares) at 60 eV.

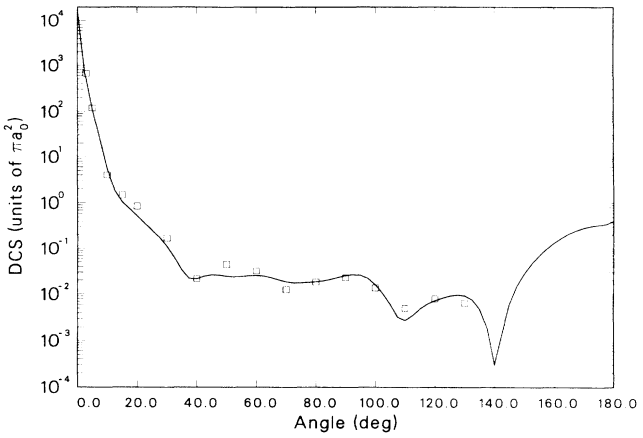

FIG. 9. Comparison of DCS's calculated with DWA (solid line) with experimental results of Jensen *et al.* (Ref. 14) (squares) at 100 eV.

with smaller amounts of other levels where the ψ_i^0's ($i = 6s6p\ ^1P_1$, $5d6p\ ^1P_1$, $6s6p\ ^3P_1$) on the right-hand side refer to pure LS-coupled states. One sees that this state is indeed dominantly an LS-coupled $^1P_1$ state.

Tables VI and VII give values of the λ and χ parameters calculated in the DWA approach. Tables VIII and IX give the same parameters calculated using FOMBT. The Fano-Macek orientation parameter[38] O_{1-} is shown graphically in Figs. 10–12 for impact electron energies of 5, 20, and 80 eV. In all three graphs the solid line represents DWA results and the dotted line represents FOMBT results. We have learned that Fabrikant[60] published EICP results for the Ba $6\,^1S$–$6\,^1P$ transition from a two-state close-coupling calculation for impact electron energy of 20 eV. These results are not, however, available to us at this time. Recently, results calculated with the present DWA approach at slightly different energies have been used to analyze some anomalies in experimental results on barium.[40]

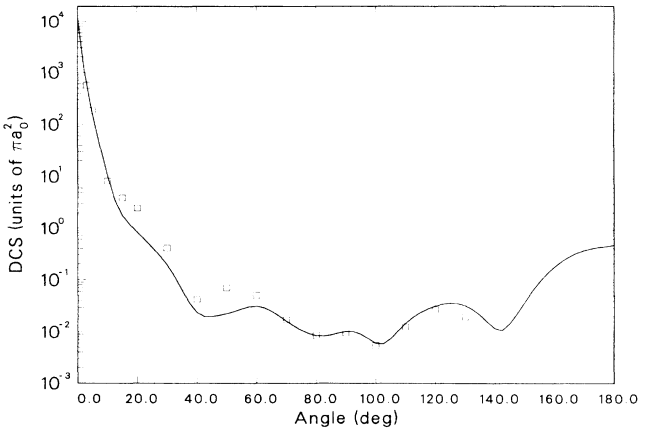

FIG. 8. Comparison of DCS's calculated with DWA (solid line) with experimental results of Jensen *et al.* (Ref. 14) (squares) at 80 eV.

IV. DISCUSSION OF RESULTS AND CONCLUSIONS

Our results for the integral and differential cross sections and for the EICP's in the case of $6s^2\,^1S_0 \rightarrow 6s6p\ ^1P_1$ excitation of barium give a comprehensive picture about the predictions of the DWA and FOMBT for this transition. As can be seen from Fig. 2, the unitarization of the scattering matrix is important for this case especially for $E < 40$ eV incident electron energies. This in turn indicates that the elements of the ρ matrix are not small[61] and thus the weak coupling approximation in its original form[62] is not applicable. The strong coupling between these two states (with an optical f value of ~ 1.59) however, justifies the negligence of couplings to other channels except for energies close to the threshold.[18] In the case of electron-impact excitation of the $3\,^1P_1$ state of magnesium, a transition similar to the one considered here (with an optical f value of ~ 1.8), it was found in general[63] that a five-state close-coupling calculation[64] gave somewhat smaller values for the DCS, especially for scattering angles $\theta > 60°$, than results from a nonunitarized FOMBT calculation.[27] Our Fig. 3 shows that even our unitarized DWA results for the integral cross sections are higher than the apparent excitation cross-section data of Chen and Gallagher.[15] It is interesting to compare our unitarized DWA and FOMBT results with the two-state ($6\,^1S, 6\,^1P$) close-coupling theory results of Fabrikant[18] which is done in our Fig. 1. As this figure shows, this close-coupling calculation gives somewhat smaller results for the integral cross section than our DWA and FOMBT calculations do for $E \geq 20$ eV incident electron energies but a substantial discrepancy with the experiment still remains for $E < 30$ eV energies. This discrepancy is further increased if the experimental values are decreased by 30% to account for cascade, as was done by Jensen *et al.* and can be seen from Fig. 1. If

TABLE VI. λ parameters calculated in the distorted-wave approximation (DWA). Column headings are electron-impact energies. Numbers in square brackets represent powers of 10.

θ \ E (eV)	5.0000	1.0000[1]	1.5000[1]	2.0000[1]	3.0000[1]	4.0000[1]	6.0000[1]	8.0000[1]	1.0000[2]
0.0000	1.0000	1.0000	1.0000	1.0000	1.0000	1.0000	1.0000	1.0000	1.0000
5.0000	8.7690[−1]	5.8526[−1]	3.5047[−1]	2.4964[−1]	1.1294[−1]	6.4259[−2]	3.4120[−2]	2.2514[−2]	1.7809[−2]
1.0000[1]	6.0054[−1]	1.7139[−1]	3.5416[−2]	3.4847[−2]	3.5838[−2]	5.6618[−2]	9.9894[−2]	1.2860[−1]	1.3661[−1]
1.5000[1]	3.2433[−1]	2.3213[−2]	2.3416[−2]	1.3935[−2]	1.3168[−1]	2.4876[−1]	3.7608[−1]	3.8163[−1]	3.6922[−1]
2.0000[1]	1.2204[−1]	7.3071[−2]	2.6916[−1]	1.0527[−1]	3.4665[−1]	4.7056[−1]	4.3980[−1]	3.3990[−1]	3.0887[−1]
2.5000[1]	3.0589[−2]	3.2447[−1]	7.5653[−1]	4.3080[−1]	5.4726[−1]	5.0790[−1]	3.4349[−1]	2.7784[−1]	2.6003[−1]
3.0000[1]	1.0212[−1]	6.4782[−1]	9.9893[−1]	8.5082[−1]	6.7999[−1]	5.1305[−1]	3.2167[−1]	1.9763[−1]	1.5402[−1]
3.5000[1]	4.0480[−1]	7.9118[−1]	9.0380[−1]	9.9756[−1]	8.3624[−1]	5.9763[−1]	2.7735[−1]	1.1033[−1]	1.1265[−1]
4.0000[1]	7.6118[−1]	7.8604[−1]	7.2384[−1]	8.9672[−1]	8.7777[−1]	7.0982[−1]	3.9974[−1]	3.0309[−1]	5.2419[−1]
4.5000[1]	7.0700[−1]	7.5492[−1]	5.4677[−1]	7.2443[−1]	7.9211[−1]	7.5052[−1]	7.7558[−1]	7.6882[−1]	6.3793[−1]
5.0000[1]	4.1050[−1]	7.4205[−1]	3.8728[−1]	5.6888[−1]	6.5074[−1]	6.7297[−1]	9.9927[−1]	8.0736[−1]	6.3829[−1]
5.5000[1]	1.9172[−1]	7.4429[−1]	2.4612[−1]	4.4677[−1]	5.2331[−1]	5.6462[−1]	9.1901[−1]	6.7805[−1]	6.0359[−1]
6.0000[1]	9.5047[−2]	7.5101[−1]	1.2982[−1]	3.4752[−1]	3.9731[−1]	4.5039[−1]	7.4839[−1]	4.6341[−1]	5.3759[−1]
6.5000[1]	8.8475[−2]	7.5115[−1]	7.2066[−2]	2.5177[−1]	2.5897[−1]	2.6413[−1]	7.3428[−1]	4.9830[−1]	4.4066[−1]
7.0000[1]	1.4462[−1]	7.3728[−1]	1.7837[−1]	1.8732[−1]	1.1967[−1]	1.8766[−2]	7.0058[−1]	4.1652[−1]	2.9406[−1]
7.5000[1]	2.4990[−1]	7.1011[−1]	5.3158[−1]	2.4838[−1]	1.5653[−1]	2.0782[−1]	8.1011[−1]	2.6629[−1]	2.1541[−1]
8.0000[1]	4.0143[−1]	6.7111[−1]	8.7130[−1]	4.3256[−1]	3.4696[−1]	4.5103[−1]	7.9042[−1]	1.9803[−1]	2.9476[−1]
8.5000[1]	5.9581[−1]	6.2561[−1]	9.7997[−1]	5.6947[−1]	4.9211[−1]	5.4107[−1]	5.6782[−1]	3.3012[−1]	4.4679[−1]
9.0000[1]	8.0751[−1]	5.7620[−1]	9.3716[−1]	6.2195[−1]	5.4731[−1]	5.5115[−1]	3.8193[−1]	5.1886[−1]	5.7504[−1]
9.5000[1]	9.6565[−1]	5.2835[−1]	8.2745[−1]	6.4597[−1]	5.8385[−1]	5.6367[−1]	3.4113[−1]	6.1721[−1]	6.3869[−1]
1.0000[2]	9.8367[−1]	4.8370[−1]	8.6765[−1]	6.4856[−1]	6.0077[−1]	5.7155[−1]	4.2092[−1]	5.7895[−1]	6.7314[−1]
1.1000[2]	6.7221[−1]	3.8495[−1]	2.0919[−1]	6.4163[−1]	6.4715[−1]	6.2031[−1]	5.6431[−1]	5.2853[−1]	6.1586[−1]
1.2000[2]	3.3819[−1]	2.6703[−1]	8.0344[−1]	7.5970[−1]	7.2734[−1]	7.1834[−1]	7.2644[−1]	7.4559[−1]	7.3418[−1]
1.3000[2]	1.2670[−1]	2.3585[−1]	9.4648[−1]	5.8835[−1]	8.5655[−1]	8.4329[−1]	8.5049[−1]	8.6141[−1]	8.9139[−1]
1.4000[2]	1.5537[−2]	3.4106[−1]	8.1346[−1]	4.7428[−1]	8.9610[−1]	9.7578[−1]	9.3560[−1]	9.3443[−1]	8.9530[−1]
1.5000[2]	2.0345[−2]	5.3059[−1]	6.7126[−1]	7.0007[−1]	6.8747[−1]	7.4045[−1]	8.5488[−1]	8.6298[−1]	8.7143[−1]
1.6000[2]	2.1501[−1]	7.5032[−1]	6.2804[−1]	8.6910[−1]	9.0398[−1]	9.1302[−1]	9.3676[−1]	9.4818[−1]	9.5058[−1]
1.7000[2]	6.6221[−1]	9.2999[−1]	8.0191[−1]	9.6615[−1]	9.7786[−1]	9.8014[−1]	9.8439[−1]	9.8853[−1]	9.9173[−1]
1.8000[2]	9.9971[−1]	9.9986[−1]	9.9996[−1]	9.9999[−1]	1.0000	1.0000	1.0000	9.9999[−1]	9.9996[−1]

TABLE VII. χ parameters calculated in the distorted-wave approximation (DWA). Column headings are electron-impact energies. Numbers in square brackets represent powers of 10.

θ \ E (eV)	5.0000	1.0000[1]	1.5000[1]	2.0000[1]	3.0000[1]	4.0000[1]	6.0000[1]	8.0000[1]	1.0000[2]
0.0000	0.0000	0.0000	0.0000	0.0000	0.0000	0.0000	0.0000	0.0000	0.0000
5.0000	−8.1841[−2]	−6.9437[−2]	9.3505[−3]	−9.1036[−2]	−2.3158[−1]	−3.7960[−1]	−6.1190[−1]	−8.4704[−1]	−8.9303[−1]
1.0000[1]	−1.1189[−1]	−1.9121[−1]	1.0550[−1]	−4.3686[−1]	−1.2186	−1.4995	−1.6664	−1.5890	−1.5189
1.5000[1]	−1.8031[−1]	−8.8318[−1]	2.7511	−1.9679	−1.8313	−1.6654	−1.2812	−9.8806[−1]	−8.1157[−1]
2.0000[1]	−3.6739[−1]	−2.4174	2.8731	−2.7270	−1.7438	−1.2378	−6.7480[−1]	−5.2633[−1]	−5.2719[−1]
2.5000[1]	−1.1755	−2.5998	2.8539	−2.9075	−1.5188	−8.8413[−1]	−4.3612[−1]	−3.5856[−1]	−4.4841[−1]
3.0000[1]	−2.3524	−2.4266	2.7054	−3.0249	−1.3326	−7.9456[−1]	−4.5514[−1]	−4.2157[−1]	−6.4809[−1]
3.5000[1]	−2.4980	−1.9981	−3.5808[−1]	1.5196	−1.0756	−7.8627[−1]	−7.5511[−1]	−1.1433	−2.1362
4.0000[1]	−2.0371	−1.6743	−4.2082[−1]	3.4000[−1]	−4.3848[−1]	−6.8573[−1]	−1.3253	−2.8467	2.3992
4.5000[1]	−1.1212	−1.5869	−5.0712[−1]	2.5640[−1]	3.5505[−2]	−3.5814[−1]	−1.9960	2.2696	1.4441
5.0000[1]	−9.0305[−1]	−1.6087	−6.3089[−1]	1.9835[−1]	1.0628[−1]	−1.7812[−1]	−6.6135[−1]	1.2154	9.4367[−1]
5.5000[1]	−1.0660	−1.6562	−8.2882[−1]	1.5799[−1]	1.0599[−1]	−1.5885[−1]	6.1622[−1]	7.2150[−1]	6.2741[−1]
6.0000[1]	−1.5347	−1.6997	−1.1854	1.5149[−1]	1.8759[−2]	−3.3876[−1]	4.2804[−1]	4.9186[−1]	4.1439[−1]
6.5000[1]	−2.1961	−1.7319	−2.0032	2.1765[−1]	4.5134[−3]	−6.2838[−1]	2.8871[−1]	3.2839[−1]	2.4927[−1]
7.0000[1]	−2.6840	−1.7708	−2.9885	5.0773[−1]	2.1894[−1]	−1.5884	−7.0681[−2]	1.4056[−1]	2.1799[−1]
7.5000[1]	−2.9809	−1.8318	2.9037	9.2193[−1]	9.5238[−1]	1.6610	−4.1013[−1]	1.1391[−1]	5.2126[−1]
8.0000[1]	3.0998	−1.9241	2.8532	9.8434[−1]	1.0109	1.1162	−5.2837[−1]	5.2297[−1]	7.8296[−1]
8.5000[1]	2.9478	−2.0421	−2.6356	7.8582[−1]	8.2695[−1]	7.5079[−1]	−5.6145[−2]	9.1624[−1]	7.8796[−1]
9.0000[1]	2.8447	−2.1797	−1.6629	5.9073[−1]	6.5199[−1]	5.5561[−1]	−9.5575[−2]	9.6461[−1]	6.9980[−1]
9.5000[1]	2.9112	−2.3304	−1.5988	4.4112[−1]	5.2513[−1]	4.4210[−1]	2.5877[−1]	9.3484[−1]	6.2502[−1]
1.0000[2]	−1.2103	−2.4803	−1.7101	3.4173[−1]	4.4731[−1]	3.9715[−1]	3.4621[−1]	1.0000	6.4738[−1]
1.1000[2]	−1.0261	−2.7664	−2.7045	3.0261[−1]	3.8261[−1]	3.7595[−1]	4.3619[−1]	6.6565[−1]	1.0822
1.2000[2]	−1.1746	3.1323	1.5093	6.4468[−1]	4.2736[−1]	4.2857[−1]	4.7390[−1]	5.7788[−1]	8.1785[−1]
1.3000[2]	−1.3014	2.5307	−4.5078[−1]	−2.3700	5.7899[−1]	4.5785[−1]	3.9184[−1]	3.5933[−1]	3.2533[−1]
1.4000[2]	−1.3562	2.0221	−9.9772[−1]	−2.1640[−1]	3.0324	2.1505[−1]	−1.9165[−2]	−1.9340[−1]	−2.3458
1.5000[2]	1.5571	1.7220	−1.0014	1.2719[−1]	6.2647[−2]	−4.2757[−1]	−1.7379[−1]	5.3738[−2]	2.0924[−1]
1.6000[2]	1.5502	1.5478	−7.7482[−1]	2.4968[−1]	2.0896[−1]	1.4013[−1]	2.1221[−1]	3.1769[−1]	4.1858[−1]
1.7000[2]	1.5242	1.4600	−4.5076[−1]	3.1655[−1]	2.3469[−1]	1.7729[−1]	1.9820[−1]	1.3453[−1]	−1.6100[−2]
1.8000[2]	0.0000	0.0000	0.0000	0.0000	0.0000	0.0000	0.0000	0.0000	0.0000

TABLE VIII. λ parameters calculated in the first-order many-body approximation (FOMBT). Column headings are electron-impact energies. Numbers in square brackets represent powers of 10.

θ \ E (eV)	5.0000	1.0000[1]	1.5000[1]	2.0000[1]	3.0000[1]	4.0000[1]	6.0000[1]	8.0000[1]	1.0000[2]
0.0000	9.9999[−1]	1.0000	1.0000	1.0000	1.0000	1.0000	1.0000	1.0000	1.0000
5.0000	8.7438[−1]	5.8875[−1]	3.3642[−1]	2.6006[−1]	1.2545[−1]	7.5714[−2]	4.3433[−2]	2.9917[−2]	2.4259[−2]
1.0000[1]	5.9148[−1]	1.7374[−1]	2.2356[−2]	3.8639[−2]	4.1454[−2]	6.4325[−2]	1.0992[−1]	1.4322[−1]	1.5444[−1]
1.5000[1]	3.0806[−1]	1.8729[−2]	4.8308[−2]	4.1995[−3]	1.2922[−1]	2.7306[−1]	4.4602[−1]	4.6982[−1]	4.6727[−1]
2.0000[1]	1.0595[−1]	7.4538[−2]	3.6714[−1]	1.1444[−1]	3.9279[−1]	5.6449[−1]	5.5276[−1]	4.5143[−1]	4.1712[−1]
2.5000[1]	3.8483[−2]	3.7752[−1]	8.0822[−1]	5.4846[−1]	6.5836[−1]	6.2546[−1]	4.5781[−1]	3.8147[−1]	3.5176[−1]
3.0000[1]	1.6238[−1]	7.5000[−1]	9.7612[−1]	9.2994[−1]	7.9564[−1]	6.3769[−1]	4.2282[−1]	2.6642[−1]	2.0248[−1]
3.5000[1]	4.3078[−1]	8.8297[−1]	9.2645[−1]	9.8822[−1]	9.1060[−1]	7.1721[−1]	3.6740[−1]	1.5982[−1]	1.9418[−1]
4.0000[1]	5.7700[−1]	8.5464[−1]	8.1048[−1]	8.9977[−1]	9.3809[−1]	8.1395[−1]	4.9509[−1]	3.8807[−1]	5.9787[−1]
4.5000[1]	4.9815[−1]	7.9858[−1]	6.7471[−1]	7.5780[−1]	8.7557[−1]	8.5186[−1]	8.0179[−1]	7.8846[−1]	6.9273[−1]
5.0000[1]	3.3863[−1]	7.5597[−1]	5.3926[−1]	6.1001[−1]	7.5314[−1]	7.8931[−1]	9.9460[−1]	8.3839[−1]	6.9022[−1]
5.5000[1]	2.0945[−1]	7.2969[−1]	4.2920[−1]	4.7391[−1]	6.2090[−1]	6.8162[−1]	9.6097[−1]	7.4830[−1]	6.7738[−1]
6.0000[1]	1.4701[−1]	7.1533[−1]	3.6291[−1]	3.4897[−1]	4.6516[−1]	5.3798[−1]	8.5628[−1]	6.5474[−1]	6.2268[−1]
6.5000[1]	1.5328[−1]	7.0818[−1]	3.4618[−1]	2.2958[−1]	2.8171[−1]	2.9880[−1]	8.3906[−1]	5.6841[−1]	4.8084[−1]
7.0000[1]	2.1988[−1]	7.0232[−1]	3.8388[−1]	1.6888[−1]	9.9364[−2]	3.4437[−2]	7.7831[−1]	4.1788[−1]	2.5878[−1]
7.5000[1]	3.3708[−1]	6.9790[−1]	4.8336[−1]	2.7412[−1]	1.2914[−1]	2.0863[−1]	8.4706[−1]	2.2884[−1]	1.8641[−1]
8.0000[1]	4.9816[−1]	6.9376[−1]	6.1399[−1]	4.7672[−1]	3.2269[−1]	4.4615[−1]	8.2502[−1]	1.7202[−1]	2.9335[−1]
8.5000[1]	6.9232[−1]	6.8768[−1]	7.0565[−1]	6.0698[−1]	4.7683[−1]	5.4375[−1]	6.3219[−1]	3.0739[−1]	4.4215[−1]
9.0000[1]	8.7625[−1]	6.7457[−1]	7.3139[−1]	6.5228[−1]	5.4108[−1]	5.5884[−1]	4.0867[−1]	4.8367[−1]	5.6109[−1]
9.5000[1]	9.4254[−1]	6.4888[−1]	7.1445[−1]	6.6366[−1]	5.8116[−1]	5.6680[−1]	3.2492[−1]	5.7052[−1]	6.3212[−1]
1.0000[2]	7.9547[−1]	6.0485[−1]	6.8168[−1]	6.5214[−1]	5.9625[−1]	5.6588[−1]	3.7656[−1]	5.2016[−1]	6.8761[−1]
1.1000[2]	3.0693[−1]	4.2828[−1]	6.4085[−1]	6.1360[−1]	6.3854[−1]	6.0584[−1]	5.3889[−1]	5.1122[−1]	6.4670[−1]
1.2000[2]	9.8028[−2]	2.0307[−1]	8.5074[−1]	7.5201[−1]	7.2277[−1]	7.0707[−1]	7.1179[−1]	7.3108[−1]	7.1360[−1]
1.3000[2]	5.7268[−2]	1.5167[−1]	9.2026[−1]	3.9871[−1]	8.6727[−1]	8.4804[−1]	8.5715[−1]	8.7334[−1]	8.9918[−1]
1.4000[2]	8.6557[−2]	2.4728[−1]	7.0362[−1]	3.3349[−1]	7.1501[−1]	9.9309[−1]	9.5030[−1]	9.4225[−1]	6.9667[−1]
1.5000[2]	1.7763[−1]	4.1150[−1]	5.9214[−1]	5.7332[−1]	5.8646[−1]	6.2474[−1]	8.2098[−1]	8.3699[−1]	8.5156[−1]
1.6000[2]	3.7204[−1]	6.3573[−1]	6.0336[−1]	7.9981[−1]	8.7020[−1]	8.7907[−1]	9.1753[−1]	9.3498[−1]	9.3935[−1]
1.7000[2]	7.2599[−1]	8.8089[−1]	7.8317[−1]	9.4655[−1]	9.7086[−1]	9.7425[−1]	9.8136[−1]	9.8728[−1]	9.9158[−1]
1.8000[2]	9.9980[−1]	9.9972[−1]	9.9998[−1]	9.9998[−1]	1.0000	1.0000	1.0000	9.9999[−1]	9.9996[−1]

TABLE IX. χ parameters calculated in the first-order many-body approximation (FOMBT). Column headings are electron-impact energies. Numbers in square brackets represent powers of 10.

θ \ E (eV)	5.0000	1.0000[1]	1.5000[1]	2.0000[1]	3.0000[1]	4.0000[1]	6.0000[1]	8.0000[1]	1.0000[2]
0.0000	0.0000	0.0000	0.0000	0.0000	0.0000	0.0000	0.0000	0.0000	0.0000
5.0000	−7.3464[−2]	−6.0487[−2]	−1.2781[−3]	−6.2675[−2]	−2.1913[−1]	−3.6542[−1]	−5.7704[−1]	−7.7551[−1]	−8.0246[−1]
1.0000[1]	−1.0344[−1]	−1.6341[−1]	3.2974[−2]	−2.5872[−1]	−1.0555	−1.3472	−1.5360	−1.4755	−1.4085
1.5000[1]	−1.7789[−1]	−8.0585[−1]	3.0525	−2.1299	−1.7679	−1.6182	−1.2530	−9.5017[−1]	−7.7158[−1]
2.0000[1]	−4.1640[−1]	−2.5841	3.0965	−3.0405	−1.7885	−1.2416	−6.2951[−1]	−4.7640[−1]	−4.9171[−1]
2.5000[1]	−1.4458	−2.7500	−3.0500	3.1146	−1.5757	−8.7561[−1]	−4.2153[−1]	−3.5550[−1]	−4.6446[−1]
3.0000[1]	−2.2183	−2.5590	−2.1297	2.9243	−1.3561	−8.0766[−1]	−5.0292[−1]	−5.0844[−1]	−7.7937[−1]
3.5000[1]	−2.1446	−1.9625	−9.5401[−1]	1.0057	−1.0900	−8.2654[−1]	−8.4890[−1]	−1.3430	−2.2345
4.0000[1]	−1.7258	−1.5157	−8.0721[−1]	4.3665[−1]	−3.7317[−1]	−7.3701[−1]	−1.4205	−2.7798	2.5764
4.5000[1]	−1.3711	−1.4280	−8.5407[−1]	3.5513[−1]	1.4265[−1]	−3.8746[−1]	−2.0960	2.4503	1.6036
5.0000[1]	−1.2973	−1.4904	−1.0077	3.0061[−1]	1.9301[−1]	−1.7436[−1]	3.1255	1.4375	1.1017
5.5000[1]	−1.4614	−1.6080	−1.2594	2.5910[−1]	1.5843[−1]	−1.7986[−1]	9.8489[−1]	9.0958[−1]	7.8472[−1]
6.0000[1]	−1.8343	−1.7455	−1.5849	2.5780[−1]	2.9004[−2]	−4.1744[−1]	5.7742[−1]	6.0846[−1]	4.9392[−1]
6.5000[1]	−2.2939	−1.8823	−1.9426	3.6680[−1]	−2.5853[−2]	−7.8389[−1]	3.0963[−1]	3.3693[−1]	2.1860[−1]
7.0000[1]	−2.6541	−2.0142	−2.3003	7.6688[−1]	1.9626[−1]	−2.0259	−1.4219[−1]	1.0299[−1]	2.0498[−1]
7.5000[1]	−2.8851	−2.1390	−2.5897	1.1843	1.1143	1.9086	−4.9757[−1]	1.5170[−1]	6.6331[−1]
8.0000[1]	−3.0219	−2.2479	−2.7323	1.1748	1.1858	1.3215	−5.5368[−1]	6.5920[−1]	9.2681[−1]
8.5000[1]	−3.0665	−2.3310	−2.7194	9.3797[−1]	9.9783[−1]	9.2575[−1]	−1.8419[−2]	1.0578	9.1176[−1]
9.0000[1]	−2.8973	−2.3829	−2.6350	7.0468[−1]	8.0796[−1]	6.9455[−1]	−9.5438[−2]	1.1302	8.3773[−1]
9.5000[1]	−1.9276	−2.4099	−2.5933	5.2556[−1]	6.5885[−1]	5.4381[−1]	2.4343[−1]	1.1603	7.9532[−1]
1.0000[2]	−1.2414	−2.4176	−2.6221	4.0416[−1]	5.6400[−1]	4.8175[−1]	3.8489[−1]	1.2292	8.4323[−1]
1.1000[2]	−1.2873	−2.4512	−2.9216	4.1572[−1]	4.8998[−1]	4.6480[−1]	5.3765[−1]	8.1913[−1]	1.2996
1.2000[2]	−1.7663	−2.7781	2.8592	1.0380	5.4246[−1]	5.1979[−1]	5.6702[−1]	6.8105[−1]	9.2386[−1]
1.3000[2]	−2.5457	2.7548	−1.8691	−2.1962	7.7606[−1]	5.7767[−1]	4.9923[−1]	4.8545[−1]	5.3286[−1]
1.4000[2]	3.0709	2.2335	−1.8904	−3.2178[−1]	3.0634	2.4290[−1]	−1.1747[−1]	−4.3545[−1]	−2.3840
1.5000[2]	2.6971	1.9675	−2.0288	1.2570[−1]	1.5066[−1]	−4.6742[−1]	−2.1416[−1]	6.7107[−2]	2.5907[−1]
1.6000[2]	2.4914	1.8063	−2.1388	2.7954[−1]	2.7388[−1]	1.6833[−1]	2.0169[−1]	3.1510[−1]	4.2195[−1]
1.7000[2]	2.3842	1.7202	−2.2064	3.5527[−1]	3.1018[−1]	2.4862[−1]	2.7787[−1]	2.4354[−1]	1.2149[−1]
1.8000[2]	0.0000	0.0000	0.0000	0.0000	0.0000	0.0000	0.0000	0.0000	0.0000

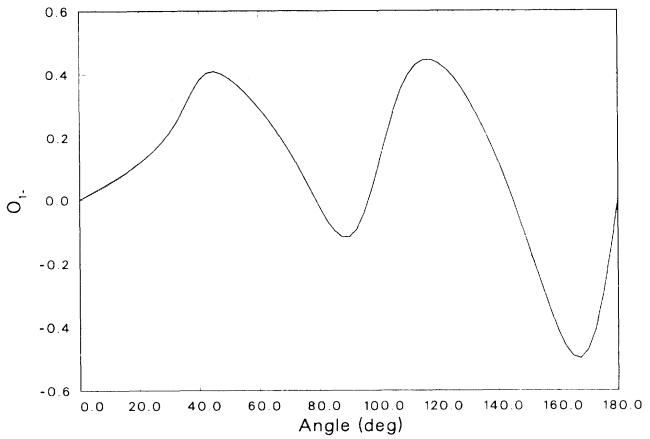

FIG. 10. Orientation parameter O_1 calculated with DWA (solid line) and FOMBT (dotted line) for electron-impact energy of 5 eV.

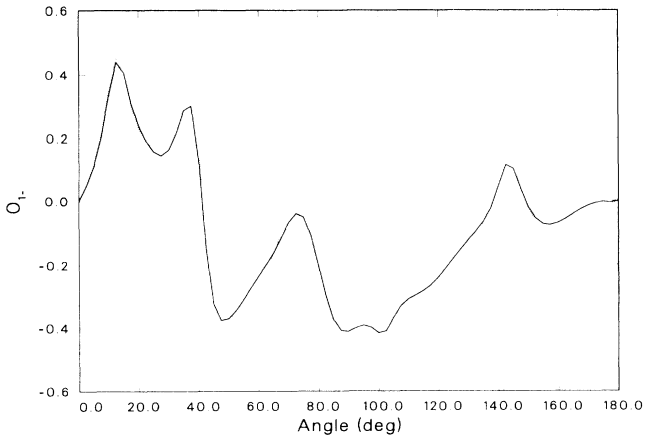

FIG. 12. Orientation parameter O_1 calculated with DWA (solid line) and FOMBT (dotted line) for electron-impact energy of 80 eV.

our DWA calculation can be trusted at 100 eV incident electron energy it seems to indicate that the 5% cascade contribution estimated by Chen and Gallagher[15] is more realistic than the 30% subtraction applied by Jensen *et al.*[14] We note here, however, that the two-state close-coupling results of Fabrikant[18] indicate a steeper decline of the integral cross section than in our case. It appears to be worthwhile to perform a close-coupling calculation for this transition for 40 eV $\leq E \leq$ 100 eV electron-impact energies in order to see to what extent the unitarization procedure accounts for the close coupling between the $6s^2\,{}^1S_0$ and $6s6p\,{}^1P_1$ states.

The comparison of our DWA results for the DCS with the experimental results of Jensen *et al.*[14] and with the theoretical results of Fabrikant[18] indicates a continuous improvement toward higher energies. Our DWA results for the DCS agree well with those of Fabrikant at 30 eV incident electron energy while the agreement is good for 20 eV energy only in the $0° \leq \theta \leq 70°$ angular range. Our results show a good agreement with the experiment (especially with respect to the shape of the DCS) in an increasing angular range. This angular range is, for 20 eV impact energy, $0° < \theta < 30°$; for 30 eV impact energy, $0° \leq \theta \leq 40°$; for 40 eV impact energy, $0° \leq \theta < 40°$; for 60 eV impact energy, $0° \leq \theta \leq 140°$, for 80 eV impact energy, $0° \leq \theta \leq 130°$; and for 100 eV impact energy, $0° \leq \theta \leq 140°$.

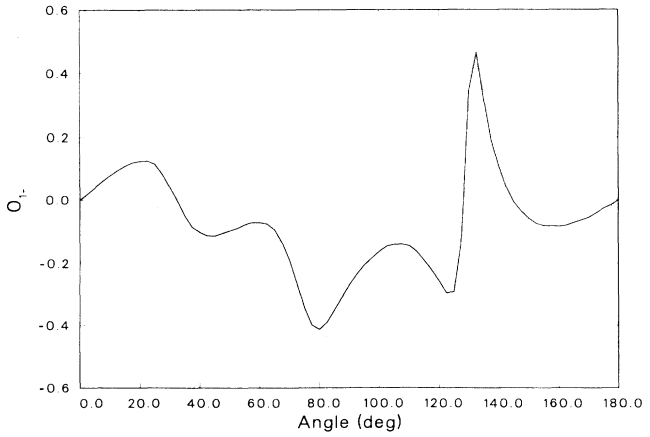

FIG. 11. Orientation parameter O_1 calculated with DWA (solid line) and FOMBT (dotted line) for electron-impact energy of 20 eV.

At 100 eV impact energy, there is an excellent quantitative agreement between theory and experiment practically over the whole angular range except our 0° value is different from the experimental extrapolated 0° cross section. This seems to indicate that the discrepancy between theory and experiment at 100 eV is not so significant as indicated by the integral cross-section result and the normalization of the experimental data due to some curious coincidence for 100 eV impact energy seems to be correct. Namely, if the experimental data would be renormalized at this energy to the present DWA results at $\theta = 5°$ or 10° scattering angles, a procedure which seems justified, there would not be any significant change in the reported experimental DCS data.

From Figs. 1–3 and 10–12 it also can be seen that there is no significant difference between the unitarized DWA and FOMBT results for the integral and differential cross sections and EICP's. This shows a certain stability of DWA schemes for such heavy atoms as barium; evidently the excitation of one or two electrons does not change significantly the distortion potential, as opposed to a small system like helium.[21,23]

As mentioned earlier, the only EICP results in the literature with which the present results can be compared are those of Fabrikant[60] which are not available to us at the present time. Our results were used for modeling the experimental data for electron scattering from the laser-excited $6\,{}^1P_1$ state of barium and good agreement with the experimentally observed intensity modulation of the superelastic scattering was obtained.[40] In comparing our DWA and FOMBT results for the EICP's as given in our Figs. 10–12 with similar results for helium it can be seen that we obtain a larger number of maxima and minima in the orientation parameter for Ba than similar calculations give for He.[26] This is evidently connected with the fact

that the orientation parameter is the result of interference among free-electron partial waves[26] and since Ba is a heavy atom there are large numbers of distorted waves that interfere with each other and thus a richer interference pattern is obtained than for helium.

The present calculation also shows that in the case of the Ba $6\,^1S_0 \rightarrow 6\,^1P_1$ transition the EICP's λ and χ change rapidly in the $0° \leq \theta < 10°$ angular range for $E \geq 60$ eV incident electron energies and therefore the extraction of these parameters for these energies appears to be a difficult experimental task.

V. CONCLUSION

Cross sections and EICP's have been calculated for the $6s^2\,^1S_0$–$6s6p\,^1P_1$ transition in neutral barium. The integral cross sections agree well with other theoretical results, but tend to be somewhat larger than experimental results. The differential cross sections show good agreement with experiment in an angular range which increases with energy. Our coherence parameters have been used to model experimental data for electrons scattering from the laser-excited $6\,^1P$ state of barium and give good agreement with the experimentally observed intensity modulation of the superelastic scattering.

ACKNOWLEDGMENTS

We thank J. B. Mann for his help in implementing the distorted-wave approximation. R. D. Cowan has provided many useful suggestions regarding the use of his Hartree-Fock computer codes. We thank S. Trajmar for many useful discussions regarding barium cross sections. D. C. Cartwright has provided help in implementing the first-order many-body approach and has given much needed general support to the entire code development effort that has made this work possible. We also thank P. Romero for cleaning up many details of the numerical work. This work was performed under the auspices of the U.S. Department of Energy.

[1]D. J. Bradley, P. Ewart, J. V. Nicholas, and J. R. D. Shaw, J. Phys. B **6**, 1594 (1973).
[2]J. L. Carlsten, T. J. McIlrach, and W. H. Parkinson, J. Phys. B **8**, 38 (1975).
[3]J. R. Rubbmark, S. A. Borgström, and K. Bockasten, J. Phys. B **10**, 421 (1977).
[4]L. Jahreiss and M. E. E. Huber, Phys. Rev. A **28**, 3382 (1983).
[5]J. L. Bowen and A. P. Thorne, J. Phys. B **18**, 35 (1985).
[6]A. Kallenbach, M. Günther, R. Künnemeyer, and M. Kock, J. Phys. B **19**, 2645 (1986).
[7]D. F. Register, S. Trajmar, S. W. Jensen, and R. T. Poe, Phys. Rev. Lett. **41**, 749 (1978).
[8]S. Trajmar, J. C. Nickel, and T. Antoni, Phys. Rev. A **34**, 5154 (1986).
[9]For a review see the recent article of F. J. Wuilleumier, D. L. Ederer, and J. L. Picqué, Adv. At. Mol. Phys. **23**, 197 (1988).
[10]L. H. Allen, *Physics of Thermal Gaseous Nebulae,* Vol. 112 of *Astrophysics and Space Science Library* (Reidel, Boston, 1984), pp. 26–30 and 116–146.
[11]*Atmospheric Physics and Chemistry,* Vol. 1 of *Applied Atomic Collision Physics,* edited by H. S. W. Massey and D. R. Bates (Academic, New York, 1982).
[12]*Gas Lasers,* Vol. 3 of *Applied Atomic Collision Physics,* edited by E. W. McDaniel and W. L. Nighan (Academic, New York, 1982).
[13]*Special Topics,* Vol. 5 of *Applied Atomic Collision Physics,* edited by H. S. W. Massey, E. W. McDaniel, and B. Bederson (Academic, New York, 1982).
[14]S. Jensen, D. Register, and S. Trajmar, J. Phys. B **11**, 2367 (1978).
[15]S. T. Chen and A. Gallagher, Phys. Rev. A **14**, 593 (1976).
[16]I. S. Aleksakhin, I. P. Zapesochnii, I. I. Garga, and V. P. Starodub, Opt. Spektrosk. **38**, 228 (1975) [Opt. Spectrosc. (USSR) **38**, 126 (1975)].
[17]I. I. Fabrikant, Atomnye Protsessy (Izol. Zinatne, Riga, 1975), p. 80.
[18]I. I. Fabrikant, J. Phys. B **13**, 603 (1980).
[19]R. J. Damburg and I. I. Fabrikant, in *Abstracts of the Ninth International Conference on the Physics of Electronic and Atomic Collisions, Seattle, 1975,* edited by J. S. Risley and R. Geballe (University of Washington, Seattle, 1975), p. 1117.
[20]J. B. Mann, At. Data Nucl. Data Tables **29**, 407 (1983).
[21]D. H. Madison and W. N. Shelton, Phys. Rev. A **7**, 499 (1973).
[22]L. D. Thomas, G. Csanak, H. S. Taylor, and B. S. Yarlagadda, J. Phys. B **7**, 1719 (1974).
[23]A. Chutjian and L. D. Thomas, Phys. Rev. A **11**, 1583 (1975).
[24]D. H. Madison, J. Phys. B **12**, 3399 (1979).
[25]D. H. Madison and K. H. Winters, J. Phys. B **16**, 4437 (1983).
[26]G. Csanak and D. C. Cartwright, Phys. Rev. A **38**, 2740 (1988).
[27]G. D. Meneses, C. B. Pagan, and L. E. Machado, in *Abstracts of the Fifteenth International Conference on the Physics of Electronic and Atomic Collisions, Brighton, 1987,* edited by J. Geddes, H. B. Gilbody, A. E. Kingston, and C. J Latimer (Queen's University, Belfast, 1987), p. 171.
[28]W. Williams and S. Trajmar, J. Phys. B **11**, 2021 (1978).
[29]M. J. Brunger, J. L. Riley, R. E. Scholten, and P. J. O. Teubner, J. Phys. B **21**, 1639 (1988).
[30]D. F. Register, S. Trajmar, S. W. Jensen, and R. T. Poe, in *Coherence and Correlation in Atomic Collisions,* edited by H. Kleinpoppen and J. F. Williams (Plenum, New York, 1980), pp. 641–650.
[31]Joseph Macek and I. V. Hertel, J. Phys. B **7**, 2173 (1974).
[32]I. V. Hertel and W. Stoll, J. Phys. B **7**, 570 (1974).
[33]I. V. Hertel and W. Stoll, J. Phys. B **7**, 583 (1974).
[34]H. W. Hermann, I. V. Hertel, W. Reiland, A. Stamatovic, and W. Stoll, J. Phys. B **10**, 251 (1977).
[35]H. W. Hermann and I. V. Hertel, in *Coherence and Correlation in Atomic Collisions,* edited by H. Kleinpoppen and J. F. Williams (Plenum, New York, 1980), p. 625.
[36]H. W. Hermann, I. V. Hertel, and M. H. Kelley, J. Phys. B **10**, 3465 (1980).
[37]For a comprehensive review on electron scattering on laser-excited targets, see I. V. Hertel and W. Stoll, Adv. At. Mol. Phys. **13**, 113 (1977).
[38]For a comprehensive review on electron-impact coherence pa-

rameters, see the recent work of N. Andersen, J. W. Gallagher, and I. V. Hertel, Phys. Rep. **165**, 1 (1988).
[39]D. F. Register, S. Trajmar, G. Csanak, S. W. Jensen, M. A. Fineman, and R. T. Poe, Phys. Rev. A **28**, 151 (1983).
[40]P. Zetner, S. Trajmar, G. Csanak, and R. E. H. Clark, Phys. Rev. A **39**, 6022 (1989).
[41]F. J. daPaixão, N. T. Padial, G. Csanak, and K. Blum, Phys. Rev. Lett. **45**, 1164 (1980).
[42]M. Eminyan, K. B. MacAdam, J. Slevin, and H. Kleinpoppen, Phys. Rev. Lett. **31**, 576 (1973); J. Phys. B **7**, 1519 (1974).
[43]J. Abdallah, Jr., R. E. H. Clark, and R. D. Cowan, Los Alamos Manual No. LA-11436-M I, 1988 (unpublished).
[44]R. E. H. Clark, J. Abdallah, Jr., G. Csanak, J. B. Mann, and R. D. Cowan, Los Alamos Manual No. LA-11436-M II, 1988 (unpublished).
[45]R. E. H. Clark, J. Abdallah, Jr., and S. P. Kramer, Los Alamos Manual No. LA-11436-M III, 1988 (unpublished).
[46]J. Abdallah, Jr. and R. E. H. Clark, Los Alamos Manual No. LA-11436-M IV, 1988 (unpublished).
[47]J. Abdallah, Jr. and R. E. Clark, Los Alamos Report No. LA-UR-89-776, 1989 (unpublished).
[48]R. D. Cowan, J. Opt. Soc. Am. **58**, 808 (1968).
[49]R. D. Cowan, J. Opt. Soc. Am. **58**, 924 (1968).
[50]R. D. Cowan and D. C. Griffin, J. Opt. Soc. Am. **66**, 1010 (1967).
[51]R. D. Cowan, *Theory of Atomic Spectra* (University of California Press, Berkeley, 1981).
[52]G. Csanak, H. S. Taylor, and R. Yaris, Phys. Rev. A **3**, 1322 (1971).
[53]G. Csanak, H. S. Taylor, and R. Yaris, Adv. At. Mol. Phys. **7**, 287 (1971).
[54]H. E. Saraph, Comput. Phys. Commun. **3**, 256 (1972).
[55]M. Rotenberg, R. Bivins, N. Metropolis, and J. K. Wooten, Jr., *The 3-j and 6-j Symbols* (Technology Press, Fairfax Station, VA, 1959).
[56]R. E. H. Clark, Comput. Phys. Commun. **16**, 119 (1978).
[57]M. K. Inal and J. Dubau, J. Phys. B **20**, 4221 (1987).
[58]W. H. Parkinson, E. M. Reeves, and F. S. Tomkins, J. Phys. B **9**, 157 (1976).
[59]B. M. Miles and W. L. Wiese, At. Data **1**, 1 (1969).
[60]I. I. Fabrikant, Izvest. Akad. Nauk. Latv. SSR, Ser. Fiz. Tekhn. **6**, 11 (1985).
[61]For a discussion on ρ matrix and unitarization, see H. Saraph, M. J. Seaton, and J. Shemming, Philos. Trans. R. Soc. London **264**, 77 (1969); J. Davis, P. C. Kepple, and M. Blaha, J. Quant. Spectrosc. Radiat. Transfer **16**, 1043 (1976); and Ref. 18.
[62]I. C. Percival and M. J. Seaton, Proc. Cambridge Philos. Soc. **53**, 654 (1957); J. M. Peek and J. B. Mann, Phys. Rev. A **16**, 2135 (1977).
[63]M. J. Brunger, J. L. Riley, R. E. Scholten, and P. J. O. Teubner, J. Phys. B **21**, 1639 (1988).
[64]I. E. McCarthy and J. D. Mitroy, J. Phys. B **22**, 641 (1989).